

Automated phase characterization and adaptive pulse compression using multiphoton intrapulse interference phase scan in air

D. Ahmadi Harris, Janelle C. Shane, Vadim V. Lozovoy, and Marcos Dantus

Department of Chemistry, Michigan State University, East Lansing, MI 48824
dantus@msu.edu

Abstract: We introduce a non-interferometric single beam method for automated spectral phase characterization and adaptive pulse compression of amplified ultrashort femtosecond pulses taking advantage of third order harmonic generation in air. This new method, air-MIIPS, compensates high-order phase distortions based on multiphoton intrapulse interference phase scan (MIIPS).

©2007 Optical Society of America

OCIS codes: (320.5540) Pulse Shaping; (320.7100) Ultrafast measurements; (320.7110) Ultrafast Nonlinear Optics;

References and links

1. A. Zewail, *Femtochemistry - Ultrafast Dynamics of the Chemical Bond*, (World Scientific, Singapore, 1994), Vols. 1 and 2.
2. A. Assion, T. Baumert, M. Bergt, T. Brixner, B. Kiefer, V. Seyfried, M. Strehle, and G. Gerber, "Control of chemical reactions by feedback-optimized phase-shaped femtosecond laser pulse," *Science* **282**, 919-922 (1998).
3. A. M. Weiner, D. E. Leaird, J. S. Patel, and J. R. Wullert, "Programmable shaping of femtosecond optical pulses by use of 128-Element Liquid-Crystal Phase Modulator," *IEEE J. Quant Electron.* **28**, 908-920 (1992).
4. R. Trebino and D. J. Kane, "Using phase retrieval to measure the intensity and phase of ultrashort pulses - frequency-resolved optical gating," *J. Opt. Soc. Am. A* **10**, 1101-1111 (1993).
5. C. Iaconis and I. A. Walmsley, "Spectral phase interferometry for direct electric-field reconstruction of ultrashort optical pulses," *Opt. Lett.* **23**, 792-794 (1998).
6. V. V. Lozovoy, I. Pastirk, and M. Dantus, "Multiphoton intrapulse interference IV: Ultrashort laser pulse spectral phase characterization and compensation," *Opt. Lett.* **29**, 775-777 (2004).
7. B. W. Xu, J. M. Gunn, J. M. Dela Cruz, V. V. Lozovoy, and M. Dantus, "Quantitative investigation of the multiphoton intrapulse interference phase scan method for simultaneous phase measurement and compensation of femtosecond laser pulses," *J. Opt. Soc. Am. B* **23**, 750-759 (2006).
8. L. T. Schelhas, J. C. Shane, and M. Dantus, "Advantages of Ultrashort phase-shaped pulses for selective two-photon activation and biomedical imaging," *Nanomedicine* **2**, 177-181 (2006).
9. S. H. Lim, A. G. Caster, O. Nicolet, and S. R. Leone, "Chemical Imaging by Single Pulse Interferometric Coherent Anti-Stokes Raman Scattering Microscopy," *J. Phys. Chem. B* **110**, 5196-5204 (2006).
10. J. M. Dela Cruz, V. V. Lozovoy, and M. Dantus, "Coherent control improves biomedical imaging with ultrashort shaped pulses," *J. Photochem. Photobio. A* **180**, 307-313 (2006).
11. V. V. Lozovoy, I. Pastirk, K. A. Walowicz, and M. Dantus, "Multiphoton intrapulse interference II: Control of two- and three-photon laser induced fluorescence with shaped pulses," *J. Chem. Phys.* **118**, 3187-3196 (2003).
12. Y. Tamaki, K. Midorikawa, and M. Obara, "Phase-matched third-harmonic generation by nonlinear phase shift in a hollow fiber," *Appl. Phys. B* **67**, 59-63 (1998).
13. C. W. Siders, N. C. Turner, M. C. Downer, A. Babine, A. Stepanov, and A. M. Sergeev, "Blue-shifted third-harmonic generation and correlated self-guiding during ultrafast barrier suppression ionization of subatmospheric density noble gases," *J. Opt. Soc. Am. B* **13**, 330-335 (1996).
14. S. Backus, J. Peatross, Z. Zeek, A. Rundquist, G. Taft, M. M. Murnane, and H. C. Kapteyn, "16-fs, 1- μ J ultraviolet pulses generated by third-harmonic conversion in air," *Opt. Lett.* **21**, 665-667 (1996).
15. V. V. Lozovoy and M. Dantus, "Systematic control of nonlinear optical processes using optimally shaped femtosecond pulses," *ChemPhysChem.* **6**, 1970-2000 (2005).
16. M. Dantus, V. V. Lozovoy, and I. Pastirk, "Measurement and repair. The femtosecond Wheatstone bridge," *OE Mag.* **3**, 15-17 (2003).
17. T. Gunaratne, M. Kangas, S. Singh, A. Gross, and M. Dantus, "Influence of bandwidth and phase shaping on laser induced breakdown spectroscopy with ultrashort laser pulses," *Chem. Phys. Lett.* **423**, 197-201 (2006).
18. J. M. Dela Cruz, V. V. Lozovoy, and M. Dantus, "Quantitative mass spectrometric identification of isomers applying coherent laser control," *J. Phys. Chem. A* **109**, 8447-8450 (2005).

19. I. Pastirk, X. Zhu, R. M. Martin, and M. Dantus, "Remote characterization and dispersion compensation of amplified shaped femtosecond pulses using MIIPS," *Opt. Express* **14**, 8885-8889 (2006).
20. I. Pastirk, B. Resan, A. Fry, J. MacKay, and M. Dantus, "No loss spectral phase correction and arbitrary phase shaping of regeneratively amplified femtosecond pulses using MIIPS," *Opt. Express* **14**, 9537-9543 (2006).
21. A. B. Fedotov, N. I. Koroteev, M. M. T. Loy, X. Xiao, and A. M. Zheltikov, "Saturation of third-harmonic generation in plasma of self-induced optical breakdown due to the self-action of 80-fs light pulses," *Opt. Comm.* **133**, 587-595 (1997).
22. Tissa C. Gunaratne, Xin Zhu, Vadim Lozovoy, Marcos Dantus, "Symmetry of nonlinear optical response to time inversion of shaped femtosecond pulses as a clock of ultrafast dynamics," *Chem. Phys.* Submitted (2007).

Introduction

Accurate measurement of the spectral phase in femtosecond laser pulses is paramount in the use of phase-modulated laser pulses for femtochemistry [1], control of chemical reactions [2], and optical communications [3]. Currently there are a number of methods for measuring the spectral phase of a femtosecond laser pulse. Frequency resolved optical gating (FROG) [4] and spectral phase interferometry for direct electric-field reconstruction (SPIDER) [5] are both interferometric multi-beam methods that utilize nonlinear optical phenomena to characterize a laser pulse's spectral phase. A recently developed single beam method, multiphoton intrapulse interference phase scan (MIIPS) [6, 7], takes advantage of the phase modulation's influence on the probability of nonlinear optical processes. This method has been shown to be very effective for accurately characterizing and compensating the spectral phase of ultrashort femtosecond pulses even as they transmit through high numerical aperture microscope objectives [7-10].

Performing MIIPS characterization and compensation using third harmonic generation (THG) in air eliminates the need for nonlinear optical crystals required for second harmonic generation. In addition, no phase-matching criterion is required for THG in air, eliminating carrier frequency and pulse bandwidth limitations of typical second harmonic generation (SHG) crystals. The influence of phase modulation on the probability of third order nonlinear processes is well understood [11]. THG has been studied in hollow-core fibers [12], in gases [13], and in air [14]. As we will demonstrate, the MIIPS method can be adapted for accurate spectral phase characterization and compensation using THG in air; yielding a new method, that we call air-MIIPS, which is very practical for characterization and optimization of amplified ultrashort pulses.

2. Theory

As in second-harmonic MIIPS [6, 7], air-MIIPS works by introducing a calibrated reference spectral phase function $f(\delta, \omega)$ to measure the unknown phase distortions $\phi(\omega)$ in the pulse. The sum of the unknown phase and the reference phase is given by $\varphi(\omega) = \phi(\omega) + f(\delta, \omega)$. The calibrated reference phase function creates a small window in the spectrum where the second derivative of the phase approaches zero, this local compensation can be written $\varphi''(\omega) = \phi''(\omega) + f''(\omega) \rightarrow 0$. As the reference function is scanned across the spectrum, the window where maximum harmonic generation takes place is scanned across the spectrum as well. For transform limited (TL) pulses, the maximum harmonic generation tracks linearly with the scanning reference phase. Deviations from the linear dependence directly provide the second derivative of the unknown phase, which can be calculated by double integration.

The reference function, $f(\delta, \omega) = \alpha \sin[\gamma\omega - \delta]$, is physically introduced with a pulse shaper. The amplitude α is set equal to π . The parameter γ , set to equal the pulse duration (full-width at half maximum), creates one window of local phase compensation across the spectrum. As the phase parameter δ is scanned the THG spectrum is recorded. Because the maximum harmonic generation occurs at the spectral position where local spectral distortions are minimal, scanning the reference phase function allows us to find $\delta_m(\omega)$, the value for which maximum harmonic intensity is measured at frequency ω . The second derivative of measured

phase can be calculated using the equation $\phi''(\omega) = \alpha \gamma^2 \sin[\gamma\omega - \delta_m(\omega)]$. The order of the nonlinear process does not matter; it may be the second harmonic as in SHG-MIIPS, THG as in this paper, or any order sum or difference frequency generation.

The second derivative of the phase, $\phi''(\omega)$, is used to calculate the desired spectral phase distortion $\phi(\omega)$ by numerical double integration over frequency. After the spectral phase distortions of the pulse are measured, the same pulse shaper is used to compensate the distortion by introducing the inverse of the measured phase $-\phi(\omega)$. Usually a single measurement results in small systematic errors which are easily corrected by iteratively compensating the phase distortions and repeating the measurement [7, 15]. Less than 10 iterations are required, for adaptive pulse compression, depending on how heavily distorted the pulse is at the start. The entire process is completed in less than one minute. The phase is measured by compensation, in analogy to the classical Wheatstone bridge used in electronics, with unprecedented accuracy. Introducing a calibrated phase with a programmable pulse shaper in order to retrieve unknown phase distortions, followed by compensating the phase distortions was proposed by our group several years ago [16]. We have used SHG-MIIPS to enhance biological imaging [10], for metal identification using laser induced breakdown spectroscopy (LIBS) [17], for isomer identification in mass spectrometry [18], and for phase correction in remote applications [19]. Now this method is simplified by means of THG in air, removing the source of possible spectral narrowing via limitation on the response function of the nonlinear crystal.

3. Experiment

Experiments were carried out with an amplified Ti:Al₂O₃ laser (Coherent, Legend USP) producing 1 mJ, 34 fs pulses at 1 kHz repetition rate. The laser amplifier was seeded with a Ti:Al₂O₃ oscillator (Coherent, Micra). The seed pulses were shaped by an all-reflective folded 4f pulse shaper with a phase only spatial light modulator (CRi SLM 128) before amplification [20].

The output laser pulse intensity was attenuated and focused in air with a concave mirror with a focal length ranging from 50 to 250 mm. For a 50 mm focal length lens and an 8 mm beam diameter, we calculate a peak power density of 2.2×10^{15} W/cm² and 8.9×10^{15} W/cm² can be attained respectively for 25 μ J and 100 μ J for TL pulses. The THG produced after the focus was collimated and separated from the fundamental beam by a fused-silica prism pair. The light was then coupled into a spectrometer (Ocean Optics USB 2000).

Figure 1 shows the SHG and THG spectra produced in a 100 μ m BBO crystal and in air respectively. Conversion efficiencies for SHG and THG were typically on the order of 10^{-2} and 10^{-4} respectively. The dashed lines represent the theoretically available bandwidth for the SHG and THG spectra; the solid lines represent the experimentally measured spectra. The reduction in bandwidth from theoretical levels, seen in the experimental second harmonic spectrum is caused by the phase matching bandwidth of the crystal which is limited by its thickness. The loss of bandwidth is absent in the THG spectrum.

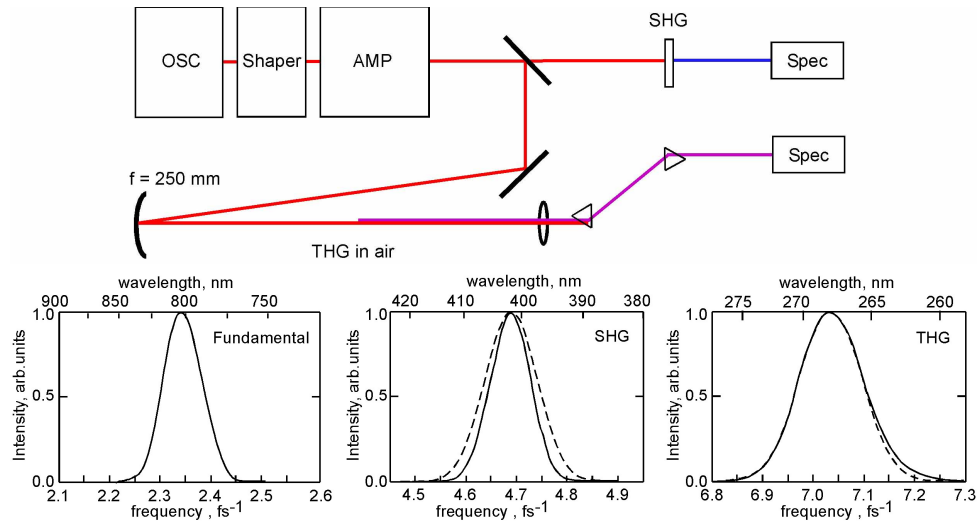


Fig. 1. (top) A schematic of the experimental setup is shown (bottom), along with the spectra for the fundamental, the SHG produced in a BBO crystal, and the THG produced in air. The dashed lines indicate the calculated SHG and THG spectra based on the fundamental spectrum and constant nonlinear susceptibilities.

For pulse intensities above $\sim 10^{13}$ W/cm², THG is accompanied by self phase modulation, self focusing, and plasma formation causing a spectral blue shift and spectral broadening in the fundamental as well as the third harmonic spectra (see Fig. 2) [21]. However, as will be shown later, during the air-MIIPS measurement, THG takes place only in a limited spectral window that is restricted by the reference phase function. The reference phase reduces the peak power density and minimizes pulse distortions. This enables air-MIIPS to be used for pulse energies where self-action effects and plasma formation would prevent phase measurements. By changing the focusing optics to a 15X reflective objective, pulse energies as low as 2 μ J were sufficient to produce sufficient signal to use air-MIIPS

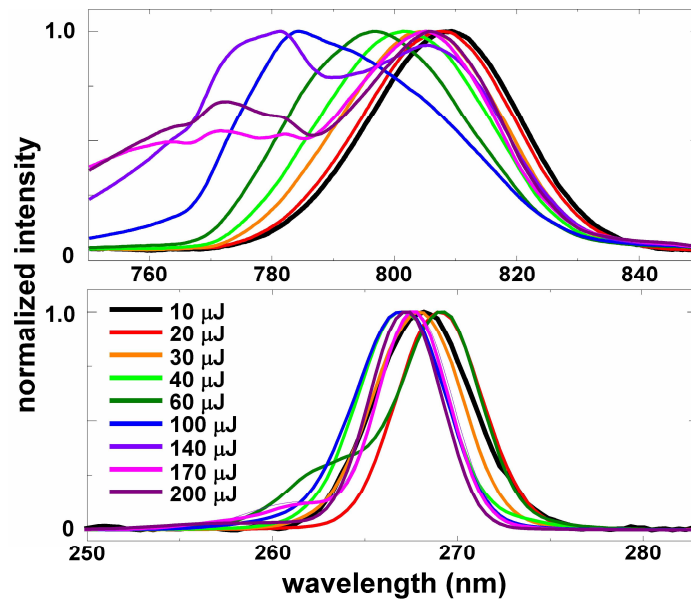


Fig. 2. Normalized intensity dependent fundamental spectrum (top) and third harmonic spectrum (bottom) after a 50 mm focal length mirror produced by transformed limited pulses.

In the data presented here, the air-MIIPS traces were produced by recording the THG spectrum as a function of the imparted sinusoidal phase shift δ . Second harmonic MIIPS (SHG-MIIPS) measurements were taken alongside the air-MIIPS measurements for the purpose of comparing the extracted phases.

4. Results

Figure 3 shows the experimental and simulated transformed limited MIIPS traces obtained for SHG-MIIPS, and for air-MIIPS. In both cases the parallel lines confirm TL pulses [12, 13]. We notice that the air-MIIPS features are broader than for SHG-MIIPS. This effect is also born out in our simulations. We also notice that in the experimental data, alternate features have different intensities, and for intense pulses, a different shape. This is caused by changes in the temporal symmetry in the shaped pulses [22]. From a technical standpoint, however, these differences are minor and have no deleterious effect on phase retrieval.

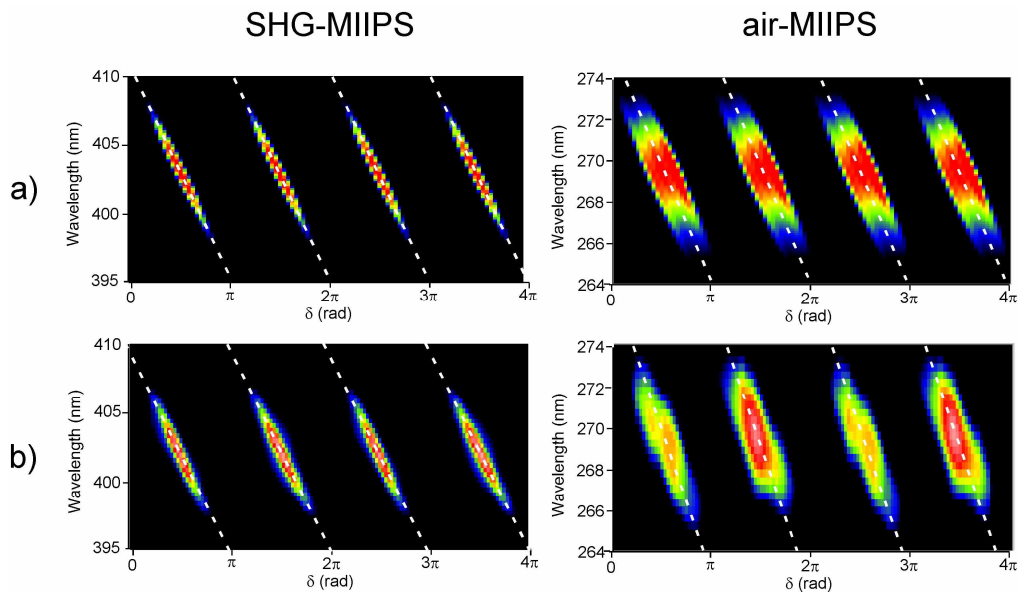


Fig. 3. (a). Theoretical SHG-MIIPS and air-MIIPS traces of transform limited pulses. (b) Experimental SHG-MIIPS and air-MIIPS traces after compensation. The dashed lines are guides to the eye and coincide with the expected location of the MIIPS features for TL pulses.

Figure 4 shows SHG-MIIPS (left) and air-MIIPS (right) traces first for initially uncompensated laser pulses, then for positive and negative chirp imparted by the pulse shaper. Although the resolution the air-MIIPS scans is lower than the SHG-MIIPS scans due to the reduced resolution of shorter wavelengths, the robust phase retrieval algorithm is still able to extract the spectral phase accurately. The performance of SHG- and air-MIIPS is compared in Fig. 5.

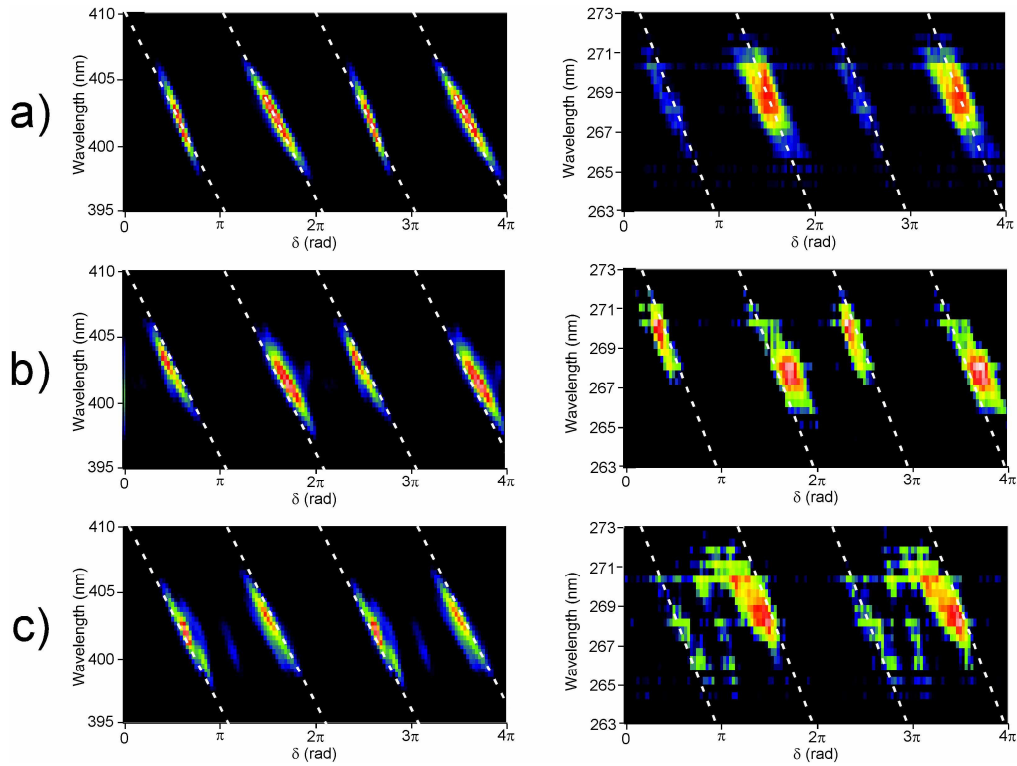


Fig. 4. SHG-MIIPS traces (left), and air-MIIPS traces (right) for a) uncompensated, b) $+2000 \text{ fs}^2$ positive chirp, and c) -2000 fs^2 negative chirp. The dashed lines are guides to the eye and coincide with the expected location of the MIIPS features for TL pulses.

Figure 5 shows the calculated spectral phase measured by SHG-MIIPS and air-MIIPS. For air-MIIPS, two representative pulse energies ($25 \mu\text{J}$ and $100 \mu\text{J}$) were chosen to be shown that correspond to energies before and after the observed self-action effects shown in Fig. 2. The calculated spectral phase from air-MIIPS is in good agreement with that of SHG-MIIPS, with residue deviations of less than 0.1 radians over the entire full width at half maximum of the laser spectrum. Moreover, the phase behavior detailing the self-action effects that characterize the strong influence of plasma formation is absent from the spectral phase extracted from air-MIIPS conducted at these plasma producing intensities. Therefore, both SHG-MIIPS and air-MIIPS are able to characterize the spectral phase of a laser pulse, and then compensate the phase with the pulse shaper.

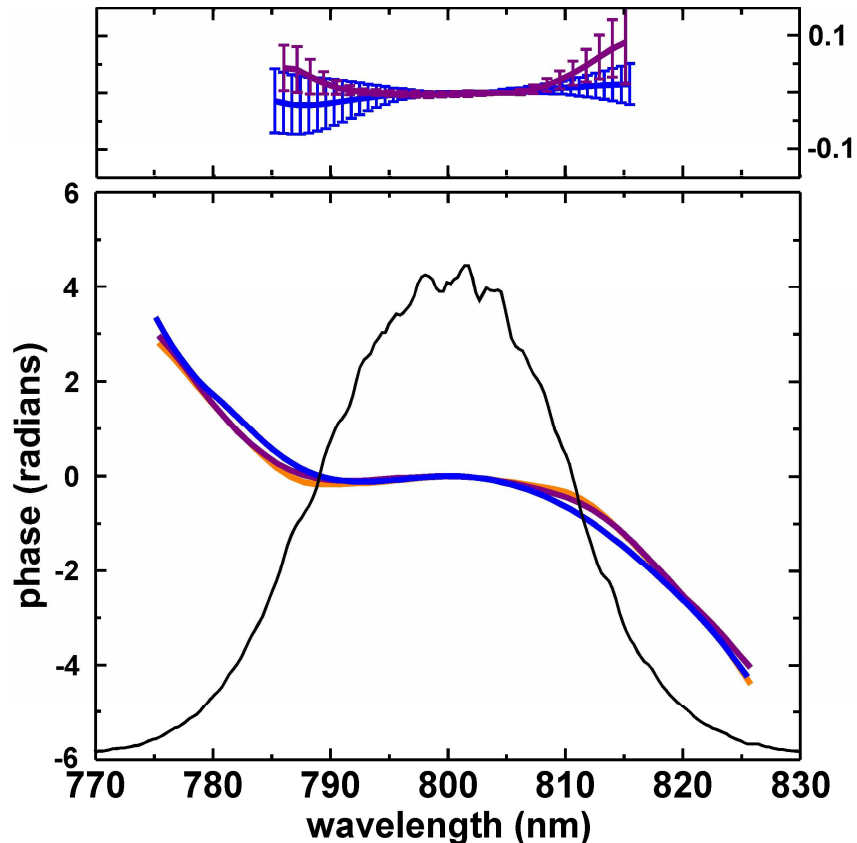


Fig. 5. Experimentally retrieved phases using SHG-MIIPS (blue) and air-MIIPS using 25 μJ (orange) and 100 μJ (purple) with a 50 mm curved mirror. (top) Residual phase distortion after compensation from SHG MIIPS (blue) and air-MIIPS (purple).

5. Conclusion

We have demonstrated an accurate phase retrieval and adaptive compensation method equivalent to SHG-MIIPS that utilizes THG in air. This third order nonlinear process is free from the bandwidth and wavelength limitations of a nonlinear crystal required for second order processes. In addition, it avoids the cost, and susceptibility to optical and environmental damage of SHG crystals.

Acknowledgments

We gratefully acknowledge funding for this research from the National Science Foundation Major Research Instrument grant CHE-0421047. D. A. Harris is grateful to the College of Natural Sciences at Michigan State University for postdoctoral funding. We also want to thank BioPhotonic Solutions Inc. for letting us use one of their pulse shapers.